Journal Name

ARTICLE

Azasilicon-Bridged Heterocyclic Arylamines: Syntheses, Structures and Photophysical Properties

Received 00th January 20xx,
Accepted 00th January 20xx

DOI: 10.1039/x0xx00000x

www.rsc.org/

Shifang Yuan[a,b,*], Lijing Wang[b], Chuanbing Huang[c], Chunxia Niu[b,c], Kai Xiang[c], Caihong Xu[c,*], Gregory A. Solan[c,d,*], Hongwei Ma[e,*], and Wen-Hua Sun[c*]

Abstract. The lithium κ^1-enamides, $Me_2NSiMe_2CHC(Ph)$-{2,6-$(R^1)_2$-4-$(R^2)C_6H_2$}NLi·3THF (R^1 = ^{i}Pr, R^2 = H **L1**; R^1 = Et, R^2 = H **L2**; R^1 = Me, R^2 = H **L3**; R^1 = R^2 = Me **L4**; R^1 = Et, R^2 = Me **L5**), in the presence of titanium tetrachloride, undergo intermolecular rearrangement cyclization reactions resulting in 1,3-migration of the silicon groups and the elimination of dimethylamine affording five examples of bis-azasilicon-bridged heterocyclic arylamines, [{2,6-$(R^1)_2$-4-$(R^2)C_6H_2$}N(Ph)$CCSiMe_2]_2$ (R^1 = ^{i}Pr, R^2 = H **D1**; R^1 = Et, R^2 = H **D2**; R^1 = Me, R^2 = H **D3**; R^1 = R^2 = Me **D4**; R^1 = Et, R^2 = Me **D5**) in good yield, respectively. The molecular structures of **D1** – **D5** show the two fused N-Si-C-C-C rings to be co-planar indicative of extended π-conjugation, while their photophysical properties reveal them to be green/blue emitting with high luminescent quantum yields (Φ_F range: 75 - 99%). Furthermore, compounds **D** serve as versatile reactants undergoing ring opening on hydrolysis to afford the saturated 1,4-diimines [2,6-$(R^1)_2$-4-$(R^2)C_6H_2$}N(Ph)C-$CH_2]_2$ (R^1 = ^{i}Pr, R^2 = H **E1**; R^1 = Et, R^2 = H **E2**; R^1 = Me, R^2 = H **E3**; R^1 = R^2 = Me **E4**; R^1 = Et, R^2 = Me **E5**). Alternatively, **D** can be employed in a redox-promoted cascade reaction to afford the conjugated 1,4-diimines, (*E*)-[{2,6-$(R^1)_2$-4-$(R^2)C_6H_2$}N=C(Ph)$CH]_2$ (R^1 = ^{i}Pr, R^2 = H **F1**; R^1 = Et, R^2 = H F**2**; R^1 = Me, R^2 = H **F3**; R^1 = R^2 = Me **F4**; R^1 = Et, R^2 = Me **F5**). In addition to **D1** – **D5**, **E1** – **E3**, **E5**, **F2** and **F3** have been the subject of single crystal X-ray diffraction studies.

Keywords: bis-azasilicon-bridged; fused heterocycles; green/blue emitting; fluorescence; organic-based devices

Introduction

π-Conjugated molecules incorporating heteroatom-bridging units have attracted widespread attention due, in large measure, to the potential applications in organic electronics and photonics.[1-9] These types of bridges not only stiffen the organic skeleton but also contribute to the electronic structure through orbital interactions which can result in fascinating properties. Indeed, significant progress has been made in the synthesis of such molecules using a variety of main-group elements.[10-16] For example, systems containing furan rings are known for their high fluorescence efficiency and good hole-transporting properties.[17-19] Elsewhere, the presence of both furan and silole moieties in the π-conjugated framework has led to extremely high fluorescence quantum yields and good thermal stability.[20,21] Moreover, the introduction of a silicon bridge can not only maintain fluorescence efficiency, comparable to that of their carbon analogs, but it can also result in improved thermal stability.[22-25] As representative examples, the bis-silicon-bridged stilbenes **A**,[26] the tetrakissilicon-bridged derivative **B**[27a,28] and the alternating Si,C-bridged **C**[27b] have been disclosed (Scheme 1). Notably, these types of compound have shown great potential as new materials for organic-based electronic devices and ambipolar carrier transporting.

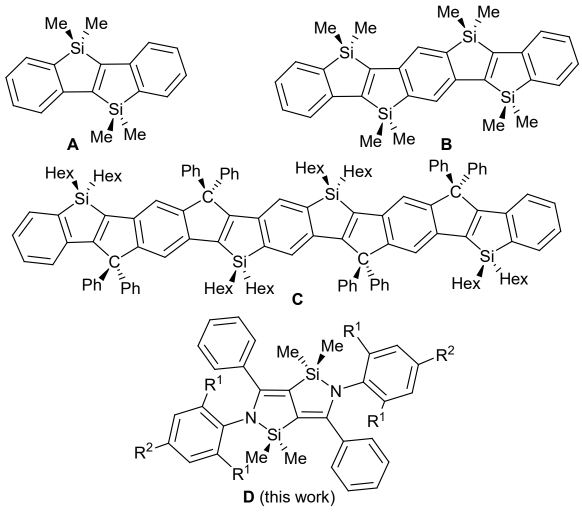

Scheme 1. Some examples of silicon-bridged π-conjugated molecules and target aza-silicon **D**.

[a] Institute of Applied Chemistry, Shanxi University, Taiyuan 030006, China. E-mail: yuansf@sxu.edu.cn
[b] The School of Chemistry and Chemical Engineering, Shanxi University, Taiyuan 030006, China
[c] Institute of Chemistry, Chinese Academy of Sciences, Beijing 100190, China. E-mail: whsun@iccas.as.cn
[d] Department of Chemistry, University of Leicester, University Road, Leicester LE1 7RH, UK. E-mail: gas8@leicester.ac.uk
[c] Analysis and Testing Centre, Beijing Institute of Technology,Beijing102488,China. E-mail: hwma@bit.edu.cn

Electronic Supplementary Information (ESI) available: CCDC 1576205 – 1576215 contain the supplementary crystallographic data for complexes **D1** – **D5**, **E1** – **E3**, **E5**, **F2** and **F3**.

As silicon possesses a 3d orbital, it can undergo conjugation with adjacent sp^2 atoms, and when in the presence of a conjugated chain it can provide a further delocalization pathway. With an imine nitrogen atom for example, the combination with a silicon-bridged π-conjugated molecule may, in principle, result in novel blue luminescent materials with fine-tuned photophysical properties and thermal stability comparable to that of their carbon analogs.[29-33] However, there are in general very few reports of conjugated molecules that contain linked but inequivalent heteroatoms[33] and, to the knowledge of the authors, no azasilicon-bridged examples reported to date; an observation likely due to the limited synthetic strategies available.

Herein, we report a novel intermolecular cyclization which employs N-arylimines as the starting materials to access a family of 3,6-diphenyl-[1,2]azasilolo[4,3-c][1,2]azasiloles, **D**, which incorporate a bis-azasilicon-bridged heterocyclic skeleton (Scheme 1). In particular, lithium κ^1-enamides, Me_2NMe_2Si-CH(Ph)C{2,6-$(R^1)_2$-4-(R^2)-C_6H_3}NLi·3THF (**L**), readily accessible from their imine precursors, are shown to undergo cyclization in the presence of a controlled amount of titanium tetrachloride leading to the target bis-azasilicon-bridged species **D**. Moreover, the fundamental photophysical properties of **D** are thoroughly investigated and correlated with the N-aryl structural variations (*viz.*, Ar = 2,6-${}^iPr_2C_6H_3$, 2,6-$Et_2C_6H_3$, 2,6-$Me_2C_6H_3$, 2,4,6-$Me_3C_6H_2$, 4-Me-2,6-$Et_2C_6H_2$); molecular structures of all examples are determined. In addition, we report the hydrolysis chemistry of **D** along with its redox-promoted reactivity leading to ring opened **E** and **F**, respectively.

Results and Discussion

Synthesis and Characterization

The lithium κ^1-enamides, $Me_2NSiMe_2CHC(Ph)$ {2,6-$(R^1)_2$-4-$R^2C_6H_2$}NLi·3THF (R^1 = ${}^iPr$, R^2 = H **L1**; R^1 = Et, R^2 = H **L2**; R^1 = Me, R^2 = H **L3**; R^1 = R^2 = Me **L4**; R^1 = Et, R^2 = Me **L5**), have been synthesized in high yield by the reaction of the corresponding N-arylimine, PhMeC=N{2,6-$(R^1)_2$-4-$R^2C_6H_2$} (R^1 = ${}^iPr$, R^2 = H; R^1 = Et, R^2 = H; R^1 = Me, R^2 = H; R^1 = R^2 = Me; R^1 = Et, R^2 = Me), using procedures previously reported (Scheme 2).[34]

Reaction of **L1 – L5** with $TiCl_4$ in a 2:1 molar ratio in THF forms [{2,6-$(R^1)_2$-4-$(R^2)C_6H_2$}N(Ph)-$CCSiMe_2$]$_2$ (R^1 = ${}^iPr$, R^2 = H **D1**; R^1 = Et, R^2 = H **D2**; R^1 = Me, R^2 = H **D3**; R^1 = R^2 = Me **D4**; R^1 = Et, R^2 = Me **D5**) in good yields (Scheme 2). These bis-azasilicon-bridged heterocycles **D** are formed as either yellow or green crystalline solids and are soluble in Et_2O or THF but sparingly soluble in CH_2Cl_2. All compounds have been characterized by ^1H and ^{13}C NMR spectroscopy and microanalysis. In addition, their molecular structures have been confirmed by single crystal X-ray diffraction.

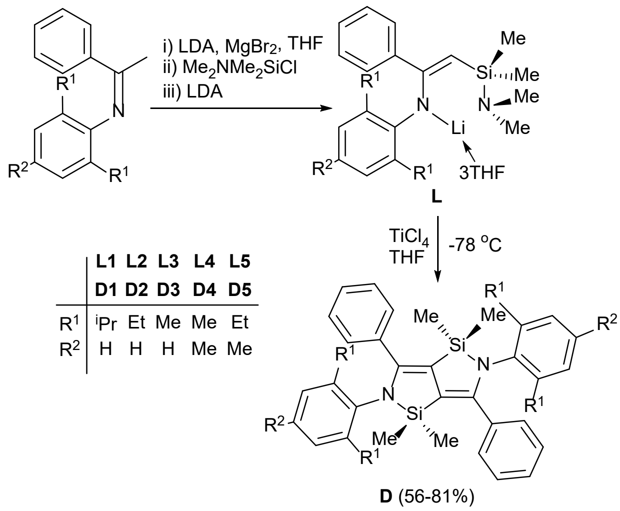

Scheme 2. Synthetic route to **D**.

Single crystals of **D1** – **D5** suitable for the X-ray determinations were grown from their dichloromethane solutions at -20 °C. Perspective views of each symmetry generated molecule are shown in Figures 1 – 5; selected bond lengths and angles are collected together in

Table 1. Selected bond distances (Å) and angles (°) for **D1** – **D5**.

	D1	**D2**	**D3**	**D4**	**D5**
Bond distances (Å)					
N-C(1)	1.424(4)	1.421(6)	1.416(3)	1.411(2)	1.412(4)
N-Si	1.770(3)	1.783(4)	1.777(2)	1.7738(13)	1.770(3)
Si-C(8^i) or Si-C(8)	1.843(3)	1.838(5)	1.840(3)	1.8448(16)	1.842(3)
C(8)-C(8^i)	1.480(6)	1.481(6)	1.485(5)	1.482(3)	1.470(6)
C(1)-C(8) or C(1)-C(8^i)	1.371(4)	1.358(7)	1.359(3)	1.359(2)	1.360(4)
Si-CH_3	1.851(4)	1.859(7)	1.852(3)	1.8548(18)	1.853(4)
	1.867(4)	1.866(6)	1.859(3)	1.8567(19)	1.857(4)
Bond angles (°)					
C(1)-N-Si	109.38(19)	111.6(3)	111.34(16)	111.58(10)	111.8(2)
N-Si-C(8^i) or N-Si-C(8)	92.78(13)	90.5(2)	90.90(10)	90.86(6)	90.55(13)
C(1)-C(8)-C(8^i) or C(1)-C(8^i)-C(8)	114.8(3)	114.0(4)	113.9(3)	114.29(17)	114.2(4)
C(1)-C(8)-Si^i C(1)-C(8^i)-Si^i	138.8(2)	136.7(4)	138.30(19)	138.29(12)	137.9(3)
C(8^i)-C(8)-Si^i or C(8)-C(8^i)-Si^i	105.6(3)	107.6(3)	107.6(2)	107.23(14)	107.7(3)
C(8)-C(1)-N or C(8^i)-C(1)-N	116.0(2)	115.4(4)	115.8(2)	115.55(13)	115.3(3)

'i' denotes elements generated by symmetry

Table 1. The structural features are similar and will be discussed together. All five structures consist of a planar core based on two five-membered heterocyclic N–Si–C–C–C rings that are fused along the C(8)–C(8^i) edge with a phenyl ring linked to each C(1) and a substituted aryl group [2,6-^{i}Pr$_2$C$_6$H$_3$ (**D1**) 2,6-Et$_2$C$_6$H$_3$ (**D2**), 2,6-Me$_2$C$_6$H$_3$ (**D3**), 2,4,6-Me$_3$C$_6$H$_2$ (**D4**), 4-Me-2,6-Et$_2$C$_6$H$_2$ (**D5**)) to each N(1). Within each five-membered ring the internal bond angles show some variation with N-C-C (115.3(3)-116.0(2)°) > C–C–C (113.9(3)-114.8(3)°) > Si–N–C (109.38(19)-111.8(2)°) > C–C–Si (105.6(3)-107.7(3)°) > C–Si–N (90.5(2)-92.78(13)°). Notably, **D1** displays the smallest Si-N-C angle and the largest N-Si-C angle of the series presumably as a consequence of steric properties imposed by the bulky N-2,6-diisopropylphenyl group. The carbon-carbon bond distances within the ring also show some differences with C(8)–C(8^i) (1.470(6)-1.485(5) Å) > C(8/8^i)–C(1) (1.358(7)-1.371(4) Å), which are consistent with the presence of partially delocalized single and double bonds, respectively. Within both rings there is some modest puckering with the N atom sitting out of the plane [dihedral angle between the N–Si–C(1) and Si–C(1)–C(8) planes is 7.84° (**D1**), 7.68° (**D2**), 6.37° (**D3**), 6.75° (**D4**), 6.69° (**D5**) (mean deviation: 0.154 Å (**D1**), 0.147 Å (**D2**), 0.089 Å (**D3**), 0.100 Å (**D4**), 0.096 Å (**D5**))]. The C-phenyl rings are inclined between 35.04° (**D1**) and 61.75° (**D5**) with respect to the plane of the fused heterocyclic core, while the N-aryl groups show a greater inclination at between 72.74° (**D1**) and 81.47° (**D5**). There are no intermolecular contacts of note.

These bis-azasilicon-bridged compounds, **D**, show some similarity to the bis-silicon-bridged stilbene **A** and the tetrakissilicon-bridged derivatives **B** and **C** with particular regard to the planarity of the structures (Scheme 1).[26–28] This would suggest, like these previously reported molecules, that the π-conjugation is effectively extended over the entire molecule. Furthermore, to the best of our knowledge, these structures are the first examples of bis-azasilicon-bridged heterocyclic arylamines.

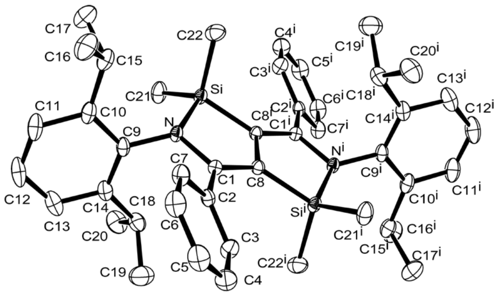

Figure 1. ORTEP representation of **D1** with the thermal ellipsoids shown at the 30% probability level; all hydrogen atoms are omitted for clarity.

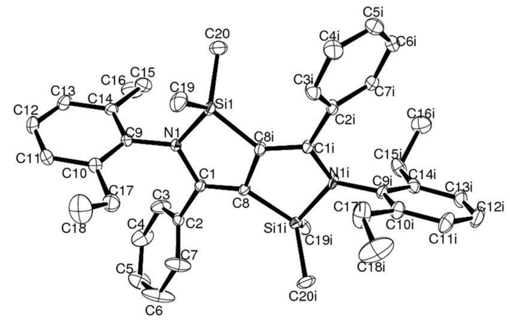

Figure 2. ORTEP representation of **D2** with the thermal ellipsoids shown at the 30% probability level; all hydrogen atoms are omitted for clarity.

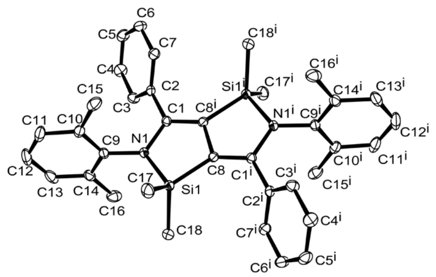

Figure 3. ORTEP representation of **D3** with the thermal ellipsoids shown at the 30% probability level; all hydrogen atoms are omitted for clarity.

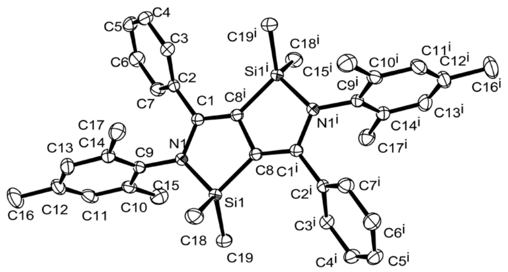

Figure 4. ORTEP representation of **D4** with the thermal ellipsoids shown at the 30% probability level; all hydrogen atoms are omitted for clarity.

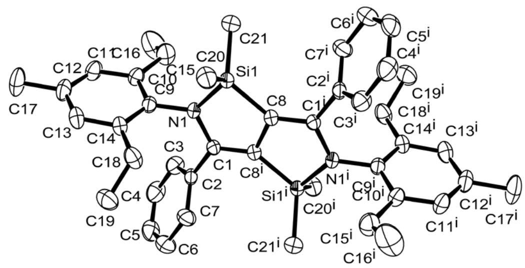

Figure 5. ORTEP representation of **D5** with the thermal ellipsoids shown at the 30% probability level; all hydrogen atoms are omitted for clarity.

Please do not adjust margins

In the [1]H NMR spectra for **D1 – D5** the Si-Me protons are seen as a 12H singlet resonance in the range δ 0.53 to – 0.03 due to their equivalent environments; similarly the [13]C NMR spectra gives a singlet for the corresponding carbons (δ 0.87 – 1.98). Within the heterocyclic rings, only two carbon signals are evident in the [13]C NMR spectra with the *C*-Ph resonance in general seen more downfield (δ 144.47 – 168.62) than the carbon atom belonging to the fused edge which is visible in a wider range (δ 65.93 – 120.29). The microanalytical data obtained for **D1** – **D5** are in agreement with their elemental compositions. Though the mechanism of formation of **D** from **L** is not explored explicitly herein, $TiCl_4$-promoted cyclizations have some precedent.[35] Nonetheless, salt elimination of lithium chloride, $TiCl_3(NMe_2)$ formation and intermolecular nucleophilic attack by the resultant anionic ArRN unit on a positively charged $RSiMe_3$ moiety with concomitant C-C bond formation seems likely.

To explore the water sensitivity of **D**, a tetrahydrofuran solution of each compound was treated with a mixture of water and THF affording, on work-up, the 1,4-diphenylbutane-1,4-diimines, 2,6-$(R^1)_2$-4-$(R^2)C_6H_2\}N(Ph)CCH_2]_2$ (R^1 = ^{i}Pr, R^2 = H **E1**; R^1 = Et, R^2 = H **E2**; R^1 = Me, R^2 = H **E3**; R^1 = R^2 = Me **E4**; R^1 = Et, R^2 = Me **E5**) (Scheme 3). Compounds **E1** – **E5** were isolated in high yields (85 **–** 90%) as colorless solids and characterized by [1]H NMR spectroscopy. All examples of **E** are novel apart from **E1** which has been recently reported albeit in low yield.[36] In addition, **E1**, **E2**, **E3** and **E5** have been the subject of single crystal X-ray diffraction studies.

Crystals of **E** suitable for the single crystal X-ray determinations were grown from their diethyl ether solutions at -20 °C. A view of **E1** is shown in Figure 6, while diagrams for **E2**, **E3** and **E5** are presented in Figures S1, S2 and S3 (see SI); selected bond distances and angles for all four structures are given in Table 2. The structures are all similar and contain an inversion center at the midpoint between C(1) and C(1^i). In each case a n-butane chain is substituted at its 1 and 4-positions by both phenyl and N-aryl groups (aryl = 2,6-$^i Pr_2C_6H_3$ (**E1**), 2,6-$Et_2C_6H_3$ (**E2**), 2,6-$Me_2C_6H_3$ (**E3**), 4-Me-2,6-$Et_2C_6H_2$ (**E5**)). Inspection of the C(2)-N(1) distance is consistent with an imine double bond (range: 1.277(2) – 1.2790(18) Å), while the N(1)-C(2)-C(1) bond angle is supportive of the expected sp^2-hybridization (range: 123.41(13) – 124.0(2)°). By contrast at C(1), the angles of between 112.07(17) and 113.99(17)° for C(2)-C(1)-C(1^i) confirm its sp^3 hybridization.

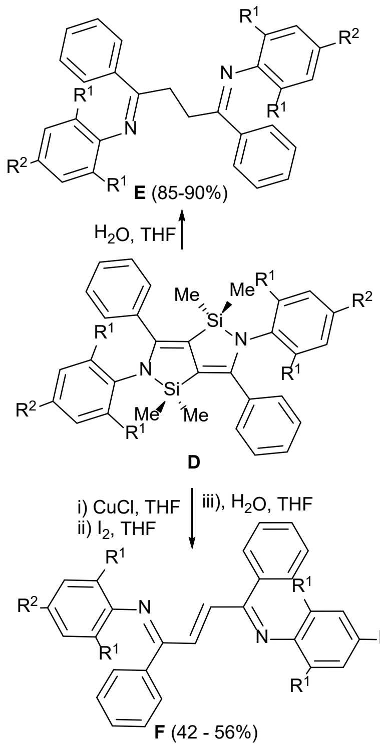

	R1	R2
E1	^{i}Pr	H
E2	Et	H
E3	Me	H
E4	Me	Me
E5	Et	Me

	R1	R2
F1	^{i}Pr	H
F2	Et	H
F3	Me	H
F4	Me	Me
F5	Et	Me

Scheme 3. Synthesis of 1,4-diimines **E** and **F**

Table 2. Selected bond distances (Å) and angles (°) for **E1**, **E2**, **E3** and **E5**

	E1	E2	E3	E5
Bond distances (Å)				
C(1)-C(1^i)	1.510(3)	1.516(3)	1.505(3)	1.536(4)
C(1)-C(2)	1.523(2)	1.5206(18)	1.502(2)	1.517(3)
C(2)-N(1)	1.278(2)	1.2790(18)	1.277(2)	1.278(3)
Bond angles (°)				
C(2)-C(1)-C(1^i)	112.07(17)	112.60(14)	113.99(17)	112.5(2)
N(1)-C(2)-C(1)	123.74(15)	123.41(13)	123.94(15)	124.0(2)
C(1)-C(2)-C(3)	118.46(14)	118.79(12)	118.38(14)	118.75(18)

'i' denotes elements generated by symmetry

The [1]H NMR data for **E** are further supportive of their structural type with a 4H singlet for the saturated N=CCH_2CH_2C=N protons at *ca.* δ 1.40 along with signals characteristic of the particular N-aryl substitution pattern. Clearly, the azasilicon compounds **E** are moisture sensitive and readily undergo C-Si bond cleavage resulting in the elimination of presumably $Me_2Si(OH)_2$ and protonation of the central carbon atoms.

We also explored the sensitivity of **D** towards redox-promoted reactivity. Hence treatment of **D** with two molar equivalents of cuprous chloride, followed by the sequential addition of four equivalents of iodine and water gives the new π-conjugated 1,4-diimines, (*E*)-[{2,6-$(R^1)_2$-4-$(R^2)C_6H_2$}N=C(Ph)-CH]$_2$ (R^1 = ^{i}Pr, R^2 = H **F1**; R^1 = Et, R^2 = H F**2**; R^1 = Me, R^2 = H **F3**; R^1 = R^2 = Me **F4**; R^1 = Et, R^2 = Me **F5**), in 42–56% yield (Scheme 3). It is assumed the reaction proceeds by ring opening of **D** to give a $ClSiMe_2$-containing intermediate which then undergoes iodination and then on hydrolysis affords **F**.[37] Compounds **F1** – **F5** have all been characterized by [1]H NMR spectroscopy and in the cases of **F2** and **F3** by single crystal X-ray diffraction.

Single crystals of **F2** and **F3** were grown from their diethyl ether solutions at -20 °C. Perspective views of **F2** and **F3** are given in Figures 7 and S4 (see SI), respectively; selected bond distances and angles for both are listed in Table 3. The structures are similar (albeit with **F3** containing an inversion center) and are based on a *E*-configured 2-butene chain with the 1- and 4-positions substituted by phenyl and by N-Ar groups (Ar = 2,6-$Et_2C_6H_3$ (**F2**), 2,6-$Me_2C_6H_3$ (**F3**)). The presence of C=C double bonds in each is supported by the bond distances of 1.292(7) (Å) (**F2**) and 1.345(5) Å (**F3**) while the C(2)-C(1)-C(1^i) angles of 127.0(6)° (**F2**) and 122.9(3)° (**F3**) support sp^2-hybridization for C(1). Furthermore, the ^1H NMR data for **F** are supportive of their structural types with a 2H singlet for the unsaturated N=CC*H*=C*H*C=N protons at *ca.* δ 5.28.

Table 3. Selected bond distances (Å) and angles (°) for **F2** and **F3**

	F2	**F3**
Bond distances (Å)		
C(1)-C(1^i)	1.292(7)	1.345(5)
C(1)-C(2)	1.500(8)	1.513(3)
C(2)-N(1)	1.265(6)	1.274(3)
Bond angles (°)		
C(2)-C(1)-C(1^i)	127.0(6)	122.9(3)
N(1)-C(2)-C(1)	126.2(5)	123.1(2)
C(1)-C(2)-C(3)	114.4(5)	119.1(2)

'i' denotes elements generated by symmetry

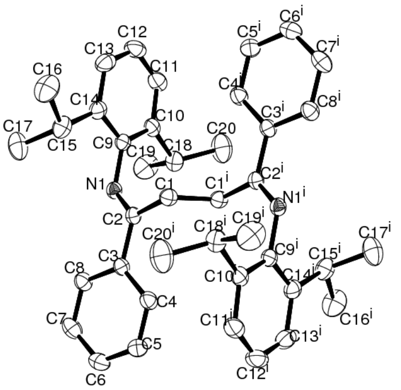

Figure 6. ORTEP representation of **E1** with the thermal ellipsoids shown at the 30% probability level; all hydrogen atoms are omitted for clarity.

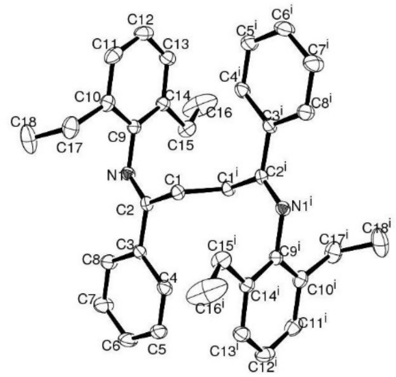

Figure 7. ORTEP representation of **F2** with the thermal ellipsoids shown at the 30% probability level; all hydrogen atoms are omitted for clarity.

Photophysical Properties of D1 – D5

The UV-vis and fluorescence spectra of **D1** – **D5** in diethyl ether solution are shown in Figures 8 and 9, respectively; the photophysical data are summarized in Table 4. Examination of the data reveals that the silicon-bridge shifts the absorption and emission maxima to a longer wavelength. Specifically, the absorption and emission maxima of **D1** – **D5** fall in the ranges 435–439 nm and 505–510 nm, respectively. These significant red shifts are attributable to the electronic contribution of the aza-atoms.[29-33] Overall, compounds **D1** – **D5** exhibit very similar absorption and emission spectra. In terms of the fluorescence quantum yields (Φ_F), **D1** – **D5** display high values in the range from 0.75 to 0.99. Notably, the 2,6-diethylphenyl-containing **D2** and the 4-methyl-2,6-diethylphenyl-containing **D5** show exceptionally high quantum yields of 0.94 and 0.99, respectively; it is unclear as to the origin of these N-aryl group influenced differences. With regard to the color of the emission, **D1** – **D5** generate an intense greenish blue emission, highlighting the potential use of these molecules as new emitting materials.

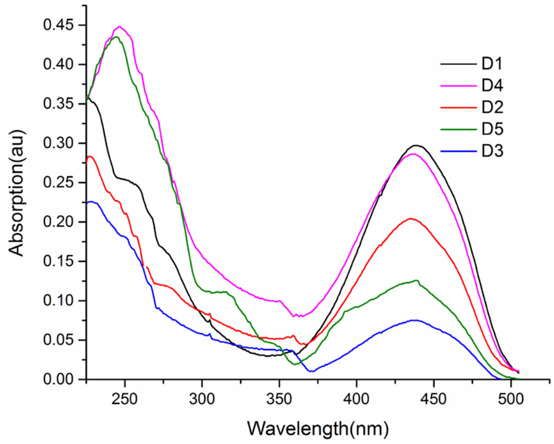

Figure 8. Normalized UV/Vis spectra of **D1** – **D5** in diethylether.

Journal Name

ARTICLE

Table 4. Photophysical properties of the azasilicon-bridged-arylamines **D**

Compound	UV–Vis absorption[a]		fluorescence[a]	
	λ_{max}/nm	log$^{\varepsilon}$	λ_{max} /nm[b]	Φ_F[c]
D1	438	4.12	515	0.81
D2	435	3.98	505	0.94
D3	437	4.02	506	0.89
D4	436	4.09	510	0.75
D5	439	4.01	510	0.99

[a] Recorded in Et_2O (2.0×10^{-5} M). [b] Emission maxima upon excitation at the absorption maximum wavelengths. [c] Determined with Rhodamine B as a standard, unless otherwise stated. The Φ_F is the average value of repeated measurements within ±5% error. [d] Determined with 9,10-diphenylanthracene as a standard. [e] Determined with anthracene as a standard.

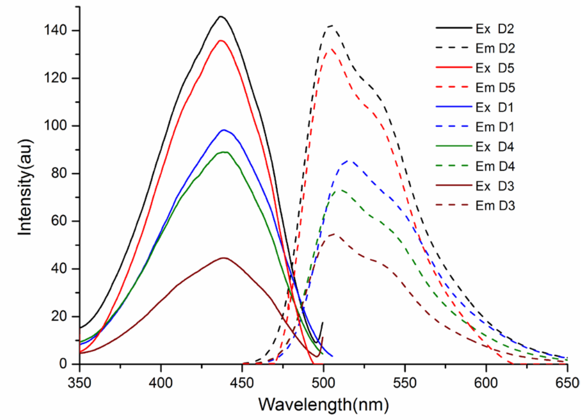

Figure 9. Fluorescence spectra of **D1 – D5** in diethylether.

Experimental

General considerations All manipulations were carried out under an atmosphere of argon using standard Schlenk techniques. Solvents were purchased from commercial sources. Deuterated solvents $CDCl_3$ were dried over activated molecular sieves (4 Å) and vacuum transferred before use. Hexane was dried using sodium potassium alloy. Diethyl ether was dried and distilled from sodium/benzophenone and stored over a sodium mirror under argon. Dichloromethane was distilled over activated molecular sieves (4 Å) or CaH_2. Toluene was heated to reflux in the presence of sodium/benzophenone and distilled under nitrogen prior to use. Glassware was oven-dried at 120 °C overnight. The NMR spectra were recorded on a Bruker DKX–600 spectrometer with TMS as the internal standard. Elemental analyses were performed with a Flash EA 1112 microanalyzer. UV/Vis absorption spectra and fluorescence spectra measurements were performed in diethyl ether at room temperature with a Shimadzu UV–757PC spectrometer and a Hitachi F–4600 fluorescence spectrophotometer, respectively. The lithium enamides, $Me_2NSiMe_2CHC(Ph)\{2,6\text{-}(R^1)_2\text{-}4\text{-}(R^2)C_6H_2\}NLi\cdot3THF$ (R^1 = ^{i}Pr, R^2 = H **L1**; R^1 = Et, R^2 = H **L2**; R^1 = Me, R^2 = H **L3**; R^1 = R^2 = Me **L4**; R^1 = Et, R^2 = Me **L5**), were prepared as bright yellow solids in high yield (90 – 98%) using procedures previously reported.[34]

Synthesis of [{2,6-(R¹)₂-4-(R²)C₆H₂}N(Ph)CCSiMe₂]₂ (D)

R^1 = ^{i}Pr, R^2 = H (D1). To a solution of **L1** (1.21 g, 2.0 mmol) in THF (25 mL) at -78 °C as added $TiCl_4$ (0.11 mL, 1.0 mmol) to form a rose solution which gradually turned brown. The mixture was stirred for 2 h at -78 °C then warmed to room temperature and kept stirring at this temperature for 24 h. All volatiles were removed under reduced pressure and the resulting residue taken up in CH_2Cl_2 (30 mL).. Following filtration, the filtrate was concentrated and recrystallized at -20 °C affording **D1** as yellow crystals (0.54 g, 81%). ^{1}H NMR (300 MHz $CDCl_3$) δ 0.12 (s, 12H, Si(CH_3)$_2$), 1.04–1.10 (d, 24H, CH(CH_3)$_2$, $^3J_{HH}$ = 6.6 Hz), 3.60 (sept, 4H, CH(CH_3)$_2$, $^3J_{HH}$ = 6.9 Hz), 6.83 (q, 2H, *p*-Ar), 6.92–6.95 (m, 4H, *m*,*p*-Ar), 7.06–7.16 (m, 6H, *p*-Ph), 7.31 (m, 4H, *m*-Ar). ^{13}C NMR (75 MHz $CDCl_3$) δ 0.87 (Si(CH_3)$_2$), 23.69 (CH_3, ^{i}Pr), 25.73, 26.68 (CH, ^{i}Pr), 115.48 (C-C), 122.02, 125.42, 127.22, 140.87 (Ph), 128.56, 146.93, 147.37 (Ar) 144.47 (C-Ph). Found: C, 78.96; H, 8.45; N, 4.18. Anal. calcd for $C_{44}H_{56}N_2Si_2$: C, 78.98; H, 8.44; N, 4.19.

R^1 = Et, R^2 = H (D2). Using a similar procedure to that described for **D1**, using **L2** (1.15 g, 2.0 mmol) and $TiCl_4$ (0.11 mL, 1.0 mmol), gave **D2** as orange crystals (0.34 g, 56%). ^{1}H NMR (300 MHz $CDCl_3$) δ 0.11 (s, 12H, Si(CH_3)$_2$), 1.16–1.18 (t, 12H, 4CH_2CH_3, $^3J_{HH}$ = 6.6 Hz), 2.74 (q, 8H, 4$CH_2$$CH_3$, $^3J_{HH}$ = 6.9 Hz), 6.89–7.07 (m, 6H, *m*, *p*-Ar), 7.25–7.42 (m, 10H, Ph). ^{13}C NMR (75 MHz $CDCl_3$) δ 1.87 (Si(CH_3)$_2$), 15.14 (CH_3, Et), 24.94 (CH_2, Et), 120.29 (C-C), 126.12–128.10 (Ar), 128.25, 138.77, 141.31, 142.97 (Ph), 156.24 (C-Ph). Found: C, 78.39; H, 7.86; N, 4.58. Anal. calcd for $C_{40}H_{48}N_2Si_2$: C, 78.37; H, 7.89; N, 4.57.

R^1 = Me, R^2 = H (D3). Using a similar procedure to that described for **D1**, using **L3** (1.09 g, 2.0 mmol) and $TiCl_4$ (0.11 mL, 1.0 mmol), gave **D3** as yellow crystals (0.40 g, 71%). ^{1}H NMR (300 MHz $CDCl_3$) δ -0.03 (s, 12H, Si(CH_3)$_2$), 1.92 (s, 12H, 4CH_3,), 6.98–7.07 (m, 6H, *m*, *p*-Ar), 7.24–7.44 (m, 10H, Ph). ^{13}C NMR (75 MHz $CDCl_3$) δ 0.59 (Si(CH_3)$_2$), 19.80 (CH_3, Me), 65.93 (C-C), 123.23, 125.52, 127.18, 167.19 (Ar), 128.65, 130.60, 137.56 (Ph), 148.14 (C-Ph). Found: C, 77.59; H, 7.27; N, 5.05. Anal. calcd for $C_{36}H_{40}N_2Si_2$: C, 77.64; H, 7.24; N, 5.03.

$R^1 = R^2$ = Me (D4). Using a similar procedure to that described for **D1**, using **L4** (1.12 g, 2.0 mmol) and $TiCl_4$ (0.11 mL, 1.0 mmol), gave **D4** as yellow-green crystals (0.38 g, 65%). ^{1}H NMR (300 MHz $CDCl_3$) δ 0.03 (s, 12H, Si(CH_3)$_2$), 0.94 (s, 18H, 6CH_3, CH_3, o/*p*-Ar), 7.19–7.22 (m, 4H, *m*-Ar), 7.51–7.68 (m, 10H, Ph). ^{13}C NMR (75 MHz $CDCl_3$) δ 1.66 (Si(CH_3)$_2$), 14.71 (s 6H, *o*-CH_3-Ar), 21.89 (s 3H, *p*-CH_3-Ar), 56.93 (C-C), 126.78, 127.84, 128.90, 130.24, 131.55, 138.74, 142.37 (Ar and Ph), 156.07 (*C*-Ph). Found: C, 78.01; H, 7.61; N, 4.78. Anal. calcd for $C_{38}H_{44}N_2Si_2$: C, 78.03; H, 7.58; N, 4.79.

R^1 = Et, R^2 = Me (D5). Using a similar procedure to that described for **D1**, using **L5** (1.18 g, 2.0 mmol) and $TiCl_4$ (0.11 mL, 1.0 mmol), gave **D5** as dark-green crystals (0.49 g, 76%). ^{1}H NMR (300 MHz $CDCl_3$) δ 0.53 (s, 12H, Si(CH_3)$_2$), 1.17–1.27 (t, 12H, 4CH_2CH_3, $^3J_{HH}$ = 7.8 Hz), 1.55–1.57 (d, 6H, CH_3, *p*-Ar, $^3J_{HH}$ = 6.3 Hz), 2.27–2.50 (q, 8H, 4C$H_2$$CH_3$, $^3J_{HH}$ = 6.9 Hz), 6.93–7.03, 7.51–7.55 (m, 14H, *m*-Ar and Ph). ^{13}C NMR (75 MHz $CDCl_3$) δ 1.98 (Si(CH_3)$_2$), 20.12 (CH_3, Et), 28.70 (CH_2, Et), 30.65 (CH_3, *p*-Ar), 72.75 (C-C), 129.82–130.02, 131.85, 133.38, 152.13, 156.04 (Ar and Ph), 168.62 (*C*-Ph). Found: C, 78.66; H, 8.17; N, 4.41. Anal. calcd for $C_{42}H_{52}N_2Si_2$: C, 78.69; H, 8.18; N, 4.37.

Synthesis of [{2,6-(R^1)$_2$-4-(R^2)C_6H_2}N(Ph)CCH_2]$_2$ (E)

General procedure. To a solution of **D** (1.0 mmol) in tetrahydrofuran (10 mL) at 0 ºC was slowly added distilled water (4-6 mmol). The resulting light yellow solution was stirred overnight and then concentrated under reduced pressure. The residue was purified on a silica gel column using petroleum ether/ether (4:1) as the eluent affording **E** (0.85 – 0.90 mmol) as colorless crystals in yields of between 85 – 90%.

R^1 = ^{i}Pr, R^2 = H (E1). ^{1}H NMR (300 MHz, $CDCl_3$) δ 1.16–1.19 (d, 24H, 4CH(CH_3)$_2$, $^3J_{HH}$ = 6.3 Hz), 1.41 (s, 4H, CH_2-CH_2), 2.85–2.89 (m, 4H, 4C*H*(CH_3)$_2$), 7.11–7.21, 7.37 –7.51, 8.05–8.06 (m, 16H, Ar and Ph). ^{13}C NMR (75 MHz $CDCl_3$) δ 22.96，23.20 (CH_3, ^{i}Pr), 28.16 (*C*H, ^{i}Pr), 29.48 (*C-C*), 127.1, 128.4, 130.4, 139.1 (Ph), 122.9, 123.3, 136.4,146.7 (Ar) 164.7 (*C*=N). Found: C, 86.36; H, 8.54; N, 5.10. Anal. calcd for $C_{40}H_{48}N_2$: C, 86.28; H, 8.69; N, 5.03.

R^1 = Et, R^2 = H (E2). ^{1}H NMR (300 MHz, $CDCl_3$) δ 1.20–1.24 (t, 12H, 4CH_2CH_3, $^3J_{HH}$ = 6.6 Hz), 1.35 (s, 4H, CH_2-CH_2), 2.43–2.47 (q, 8H, 4C$H_2$$CH_3$, $^3J_{HH}$ = 6.9 Hz), 6.90–7.03, 7.41–7.52, 8.01–8.03 (m, 16H, Ar and Ph). ^{13}C NMR (75 MHz $CDCl_3$) δ 14.14 (CH_3, Et), 23.84 (CH_2, Et), 29.29 (*C-C*), 128.1, 128.3, 131.2, 137.5 (Ph), 120.6, 124. 6, 133.8,149.6 (Ar) 164.6 (*C*=N). Found: C, 86.46; H, 8.01; N, 5.52. Anal. calcd for $C_{36}H_{40}N_2$: C, 86.35; H, 8.05; N, 5.59.

R^1 = Me, R^2 = H (E3). ^{1}H NMR (300 MHz, $CDCl_3$) δ 2.02–2.05 (d, 12H, CH_3, *p*-Ar, $^3J_{HH}$ = 6.9 Hz), 1.47 (s, 4H, CH_2-CH_2), 7.04–7.11, 7.35–7.46, 7.99–8.02 (m, 16H, Ar and Ph). ^{13}C NMR (75 MHz $CDCl_3$) δ 18.19 (CH_3, Me), 29.23 (*C-C*), 128.2, 128.6, 131.0, 137.5 (Ph), 127.0, 128. 3, 131.8, 153.2 (Ar), 164.7 (*C*=N). Found: C, 86.37; H, 7.24; N, 6.38. Anal. calcd for $C_{32}H_{32}N_2$: C, 86.44; H, 7.25; N, 6.30.

$R^1 = R^2$ = Me (E4). ^{1}H NMR (300 MHz, $CDCl_3$) δ 2.04–2.06 (d, 18H, CH_3, *p*-Ar, $^3J_{HH}$ = 6.9 Hz), 1.54 (s, 4H, CH_2-CH_2), 6.86–6.88, 7.39–7.46, 8.01–8.04 (m, 14H, Ar and Ph). ^{13}C NMR (75 MHz $CDCl_3$) δ 19.98 (s 6H, *o*-CH_3-Ar), 24.19 (s 3H, *p*-CH_3-Ar), 29.34 (*C-C*), 128.8, 129.2, 131.5, 133.1 (Ph), 126.5, 128.9, 129.6, 146.2 (Ar), 164.6 (*C*=N). Found: C, 86.47; H, 7.64; N, 5.90. Anal. calcd for $C_{34}H_{36}N_2$: C, 86.40; H, 7.68; N, 5.93.

R^1 = Et, R^2 = Me (E5). ^{1}H NMR (300 MHz, $CDCl_3$) δ 1.13–1.21 (t, 12H, 4CH_2CH_3, $^3J_{HH}$ = 7.8 Hz), 2.29–2.31 (d, 6H, CH_3, *p*-Ar, $^3J_{HH}$ = 6.3 Hz), 1.52 (s, 4H, CH_2-CH_2), 2.56–2.61 (q, 8H, 4C$H_2$$CH_3$, $^3J_{HH}$ = 6.3 Hz), 6.94–7.20, 7.61–7.67, 8.03–8.06 (m, 14H, Ar and Ph). ^{13}C NMR (75 MHz $CDCl_3$) δ 19.18 (CH_3, Et), 24.70 (CH_3, *p*-Ar), 28.35 (CH_2, Et), 29.40 (*C-C*), 128.2, 128.5, 131.8, 136.4 (Ph), 128.5, 133.6, 136.8, 147.6 (Ar), 164.7 (*C*=N). Found: C, 86.35; H, 8.32; N, 5.33. Anal. calcd for $C_{38}H_{44}N_2$: C, 86.31; H, 8.39; N, 5.30.

Synthesis of (*E*)-[{2,6-(R^1)$_2$-4-(R^2)C_6H_2}N=C(Ph)CH]$_2$ (F)

General procedure. To a solution of **D** (2.0 mmol) in THF (25 mL) at -78 ºC, CuCl (4.0 mmol) was added to form a yellow-green solution which gradually turned to a black green. The mixture was stirred for 3 h at -78 ºC then warmed to room temperature and left to stir at this temperature for 24 h. All volatiles were removed under reduced pressure and the residue taken up in CH_2Cl_2 (50 mL). The solution was filtered and all volatiles removed from the filtrate under reduced pressure. The resulting residue was cooled to -78 ºC and four equivalents of I_2 (8.0 mmol) in THF (30 mL) added resulting in a color change to brown. The reaction mixture was stirred for 3 h at -78 ºC, then warmed to room temperature and left to stir at this temperature for 24 h. All volatiles were removed under reduced pressure and the resulting residue taken up in diethyl ether (30 mL) and filtered. The filtrate was cooled to 0 ºC and distilled water (8–10 mmol) slowly added. The resulting solution was stirred overnight at room temperature. The brown solution was concentrated under reduced pressure and the residue purified on a silica gel column using petroleum ether/diethylether (4.5:1) as eluent to afford **F** in yields of between 42–56%; recrystallization from diethyl ether at 20 ºC formed **F** as colorless crystals.

R^1 = ^{i}Pr, R^2 = H (F1). ^{1}H NMR (300 MHz, $CDCl_3$) δ 1.14–1.17 (d, 24H, 4CH(CH_3)$_2$, $^3J_{HH}$ = 6.3 Hz), 2.79–2.81 (m, 4H, 4C*H*(CH_3)$_2$), 5.26 (s, 2H, C*H*=C*H*), 7.09–7.16, 7.39–7.52, 8.03–8.07 (m, 16H, Ar and Ph). ^{13}C NMR (75 MHz $CDCl_3$) δ 22.96, 23.20 (CH_3, ^{i}Pr), 28.16 (*C*H, ^{i}Pr), 124.3 (*C*=*C*), 127.1, 128.4, 130.4, 139.1 (Ph), 122.9, 123.3, 136.1 (Ar) 164.7 (*C*=N). Found: C, 86.48; H, 8.44; N, 5.08. Anal. calcd for $C_{40}H_{46}N_2$: C, 86.59; H, 8.36; N, 5.05.

R^1 = Et, R^2 = H (F2). ^{1}H NMR (300 MHz, $CDCl_3$) δ 1.21–1.24 (t, 12H, CH_2CH_3, $^3J_{HH}$ = 6.6 Hz), 2.65–2.69 (q, 8H, C$H_2$$CH_3$, $^3J_{HH}$ = 6.9 Hz), 5.32 (s, 2H, C*H*=C*H*), 6.91–7.03, 7.41–7.52, 8.02–8.05 (m, 16H, Ar and Ph). ^{13}C NMR (75 MHz $CDCl_3$) δ 14.14 (CH_3, Et), 23.84 (CH_2, Et), 124.2 (*C*=*C*), 128.1, 128.3, 131.2, 137.5 (Ph), 120.6, 124. 6, 133.8,149.6 (Ar) 164.6 (*C*=N). Found: C, 86.64; H, 7.72; N, 5.64. Anal. calcd for $C_{36}H_{38}N_2$: C, 86.70; H, 7.68; N, 5.62.

R^1 = Me, R^2 = H (F3). ^{1}H NMR (300 MHz, $CDCl_3$) δ 2.03–2.05 (d, 12H, CH_3, *p*-Ar, $^3J_{HH}$ = 6.9 Hz), 5.30 (s, 2H, C*H*=C*H*), 7.01–7.11, 7.36–7.46, 8.01–8.04 (m, 16H, Ar and Ph). ^{13}C NMR (75 MHz $CDCl_3$) δ 18.19 (CH_3, Me), 124.3 (*C*=*C*), 128.2, 128.6, 131.0, 137.5 (Ph), 127.0, 128. 3, 131.8,153.2 (Ar) 164.7 (*C*=N). Found: C, 86.79; H, 6.84; N, 6.37. Anal. calcd for $C_{32}H_{30}N_2$: C, 86.84; H, 6.83; N, 6.33.

$R^1 = R^2$ = Me (F4). ^{1}H NMR (300 MHz, $CDCl_3$) δ 2.03–2.06 (d, 18H, CH_3, *p*-Ar, $^3J_{HH}$ = 6.9 Hz), 5.28 (s, 2H, C*H*=C*H*), 6.82–6.87, 7.42–7.46, 8.00–8.07 (m, 14H, Ar and Ph). ^{13}C NMR (75 MHz $CDCl_3$) δ 19.98 (s

6H, *o*-CH_3-Ar), 24.19 (s 3H, *p*-CH_3-Ar), 124.3 (*C*-*C*), 128.8, 129.2, 131.5, 133.1 (Ph), 126.5, 128.9, 129.6, 146.2 (Ar), 164.6 (*C*=N). Found: C, 86.67; H, 7.34; N, 5.98. Anal. calcd for $C_{34}H_{34}N_2$: C, 86.77; H, 7.28; N, 5.95.

R^1 = Et, R^2 = Me (F5). ^{1}H NMR (300 MHz, $CDCl_3$) δ 1.18–1.23 (t, 12H, 4CH_2CH_3, $^3J_{HH}$ = 7.8 Hz), 2.30–2.33 (d, 6H, CH_3, *p*-Ar, $^3J_{HH}$ = 6.3 Hz), 2.58–2.62 (q, 8H, 4CH_2CH_3, $^3J_{HH}$ = 6.3 Hz), 5.29 (s, 2H, C*H*=C*H*), 6.98–7.25, 7.53–7.66, 8.04–8.06 (m, 14H, Ar and Ph). ^{13}C NMR (75 MHz $CDCl_3$) δ 19.18 (*C*H_3, Et), 24.70 (*C*H_3, *p*-Ar), 28.35 (*C*H_2, Et), 124.2 (*C*=*C*), 128.2, 128.5, 131.8, 136.4 (Ph), 128.5, 133.6, 136.8, 147.6 (Ar), 164.7 (*C*=N). Found: C, 86.67; H, 8.02; N, 5.31. Anal. calcd for $C_{38}H_{42}N_2$: C, 86.64; H, 8.04; N, 5.32.

X-ray Crystallographic Studies. Single crystal X-ray diffraction data for **D1** – **D5**, **E1**, **E2, E3**, **E5**, **F2** and **F3** were collected using Mo-Kα radiation (*λ* = 0.71073 Å) on a Bruker ApexII CCD diffractometer and Rigaku AFC 10 Saturn724 in the range 173(2) K to 293(2) K. Crystals were coated in oil and then directly mounted on the diffractometer under a stream of cold nitrogen gas. Cell parameters were obtained by global refinement of the positions of all collected reflections. Intensities were corrected for Lorentz and polarization effects and empirical absorption. The structures were solved by direct methods and refined by full-matrix least squares on F^2. All hydrogen atoms were placed in calculated positions. Structure solution and refinement were performed by using the SHELXL-2014 package and Olex2 1.2 package.[38] The remaining non-hydrogen atoms were then obtained from the successive difference Fourier maps. All non−H atoms were refined with anisotropic displacement parameters, while the H atoms were constrained to parent sites, using riding modes (SHELXTL).[39] Crystal data and processing parameters for **D1** – **D5** are summarized in Table 5, while those for **E1**, **E2, E3**, **E5**, **F2** and **F3** are presented in Table 6.

Table 5. Crystal data and data collection parameters for **D1 – D5**

compound	**D1**	**D2**	**D3**	**D4**	**D5**
CCDC No.	1576205	1576206	1576207	1576208	1576209
formula	$C_{44}H_{56}N_2Si_2$	$C_{40}H_{48}N_2Si_2$	$C_{36}H_{40}N_2Si_2$	$C_{38}H_{44}N_2Si_2$	$C_{42}H_{52}N_2Si_2$
fw	669.08	612.98	556.88	584.93	639.52
T, K	213(2)	200(2)	173(2)	200(2)	200(2)
cryst syst	Triclinic	Monoclinic	Monoclinic	Monoclinic	Monoclinic
space group	P-1	Pn	P2(1)/c	P2(1)/c	P2(1)/c
a, Å	8.234(7)	12.4574(14)	10.093(2)	10.7045(12)	10.558(3)
b, Å	9.416(6)	13.7387(13)	12.721(3)	12.8727(15)	13.688(5)
c, Å	13.972(11)	20.538(2)	11.827(2)	11.9991(14)	12.845(4)
α, °	82.68(5)	90	90	90	90
β, °	76.62(7)	95.175(2)	92.34(3)	92.607(2)	90.115(6)
γ, °	69.13(7)	90	90	90	90
V, Å^3	983.5(14)	3500.8(6)	1517.1(5)	1651.7(3)	1856.4(10)
μ/mm^{-1}	0.122	0.131	0.145	0.136	0.126
Z	1	4	4	2	2
ρ_{calc}, g/cm^3	1.130	1.162	1.219	1.176	1.144
ϑ range (°)	2.70–25.01	2.88–28.26	2.02–27.48	1.90–25.04	1.93-25.05
index ranges	-9≤h≤3 -11≤k≤10 -15≤l≤16	-16≤h≤16 -17≤k≤18 -26≤l≤27	-13≤h≤13 -16≤k≤16 -15≤l≤15	-12≤h≤12 -15≤k≤15 -14≤l≤14	-12≤h≤5 -16≤k≤16 -15≤l≤15
No. of reflns collected	3581	31335	10692	17243	7939
No. of unique reflns [R_{int}]	3226 [0.0151]	15420 [0.0387]	3470 [0.0527]	2920 [0.0315]	3286 [0.0623]
No. of parameters	223	793	185	195	215
GOF on F^2	1.043	1.037	1.035	1.029	1.003
F(000)	362	1318	596	628	689
Completeness to θ (%)	93.2	99.7	99.7	99.9	100
Final *R* indices (I>2σ(I))	R1 = 0.0684, wR2 = 0.2201	R1 = 0.0700, wR2 = 0.1871	R1 = 0.0686, wR2 = 0.2064,	R1 = 0.0360, wR2 = 0.0990	R1 = 0.0614, wR2 = 0.1629
R indices (all data)	R1 = 0.0807, wR2 = 0.2512	R1 = 0.0839, wR2 = 0.2000	R1 = 0.0796, wR2 = 0.2209,	R1 = 0.0439, wR2 = 0.1068	R1 = 0.1062, wR2 = 0.1931
Largest diff peak/hole, e Å^3	0.54/-0.40	0.98/-0.43	0.42/-0.34	0.23/-0.23	0.51/-0.40

Table 6. Crystal data and data collection parameters for **E1 - E3, E5, F2** and **F3**

complex	E1	E2	E3	E5	F2	F3
CCDC No.	1576210	1576211	1576212	1576213	1576214	1576215
formula	$C_{40}H_{48}N_2$	$C_{36}H_{40}N_2$	$C_{32}H_{32}N_2$	$C_{38}H_{44}N_2$	$C_{36}H_{38}N_2$	$2(C_{32}H_{30}N_2)$
fw	556.80	500.70	444.59	528.75	498.68	885.16
T, K	223(2)	200(2)	200(2)	296(2)	200(2)	296(2)
cryst syst	Monoclinic	Triclinic	Triclinic,	Triclinic	Monoclinic	Triclinic
space group	P2(1)/n	P-1	P-1	P-1	P2(1)/n	P-1
a, Å	8.839(3)	8.3622(4)	10.2057(10)	8.181(2)	9.937(3)	10.129(2)
b, Å	12.054(4)	8.7201(5)	11.4873(11)	9.014(2)	13.257(4)	11.495(3)
c, Å	16.055(7)	11.3838(6)	12.1715(11)	11.892(4)	22.000(7)	12.113(3)
α, °	90	69.821(2)	66.232(2)	86.414(6)	90	66.334(5)
β, °	100.70(4)	81.103(2)	83.013(2)	70.448(5)	96.887(7)	82.721(4)
γ, °	90	70.285(2)	83.378(2)	69.436(4)	90	83.176(5)
V, Å^3	1680.8(11)	732.79(7)	1292.8(2)	772.2(4)	2877.4(16)	1277.6(5)
μ/mm^{-1}	0.063	0.065	0.066	0.065	0.066	0.067
Z	2	1	4	1	4	1
ρ_{calc}, g/cm^3	1.100	1.135	1.142	1.137	1.151	1.150
ϑ range (°)	2.13–25.00	3.07–25.04	1.834–25.049	1.82–25.04	1.797–28.193	1.99–25.049
index ranges	-10≤h≤7 -14≤k≤14 -19≤l≤14	-9≤h≤9 -7≤k≤10 -13≤l≤13	-12≤h≤11 -13≤k≤6 -14≤l≤12	-8≤h≤9 -10≤k≤10 -7≤l≤14	-8≤h≤11 -15≤k≤14 -26≤l≤26	-12≤h≤11 -13≤k≤10 -14≤l≤11
No. of reflns collected	5656	5599	7223	4360	15985	7175
No. of unique reflns [R_{int}]	2857 [0.0293]	2530 [0.0253]	4556 [0.0169]	2738 [0.0234]	5167 [0.1380]	4526 [0.0321]
No. of parameters	194	175	312	185	371	312
GOF on F^2	1.039	1.026	1.022	1.033	0.947	1.027
F(000)	604.0	270.0	476.0	286.0	1072.0	472.0
Completeness to θ (%)	96.2	97.7	99.3	99.9	100.0	99.9
Final *R* indices (I>2σ(I))	R1 = 0.0502, wR2 = 0.1244	R1 = 0.0576, wR2 = 0.1491	R1 = 0.0430, wR2 = 0.1020	R1 = 0.0562, wR2 = 0.1425	R1 = 0.0794, wR2 = 0.1934	R1 = 0.0537, wR2 = 0.1300
R indices (all data)	R1 = 0.0716, wR2 = 0.1380	R1 = 0.0726, wR2 = 0.1615	R1 = 0.0648, wR2 = 0.1158	R1 = 0.0883, wR2 = 0.1632	R1 = 0.2371, wR2 = 0.2926	R1 = 0.1004, wR2 = 0.1531
Largest diff peak/hole, e Å^3	0.15/-0.16	0.73/-0.40	0.14/-0.14	0.26/-0.20	0.30/-0.27	0.42/-0.35

Conclusions

In summary, we have developed a new class of highly fluorescent azasilicon-containing π-electron compounds that have potential as blue-emitting materials for use as organic light-emitting diodes (LEDs). In particular, the bis-azasilicon-bridged heterocycles **D1 – D5**, that differ in the nature of the N-aryl group, have been prepared via an intermolecular cyclization route involving the reaction of the corresponding lithium κ^1-enamide with titanium tetrachloride. In terms of their photophysical properties, the presence of the silicon bridge significantly shifts both the absorption and emission maxima to a longer wavelength.[27a] Furthermore, all the bis-azasilicon-bridged heterocyclic arylamines display high fluorescence efficiency that is to some degree influenced by the N-aryl group; moreover their range in quantum yields exhibited by **D1** – **D5** is comparable to that observed for the previously reported bis-silicon-bridged stilbenes (Figure 1). We have also found that **D** can serve as precursors to saturated (**E**) and unsaturated 1,4-diimines (**F**), the latter involving cascade redox reactions. Overall, we consider the amenability to structural modification in **D** at not just the aryl positions but also the silicon moiety offers a convenient future means to construct new π-conjugated systems based on the bis-azasilicon-bridged skeleton; materials that may have a range of applications including as organic-based electronic and optoelectronic devices.

Acknowledgements

The authors thank the National Natural Science Foundation of China (Nos 21101101 and U1362204) and Shanxi Province Natural Science Fund (No. 2012021007-1) for financial support. We also thank the Scientific Instrument Center of Shanxi University. GAS thanks the Chinese Academy of Sciences for a Visiting Fellowship.

Notes and references

1 A. K. Mishra, M. Graf, F. Grasse, J. Jacob, E. J. W. List, K. Müllen, *Chem. Mater*. 2006, **18**, 2879.

2 P. T. Boudreault, S. Wakim, N. Blouin, M. Simard, C. Tessier, Y. Tao, M. Leclerc, *J. Am. Chem. Soc.* 2007, **129**, 9125.
3 H. Ebata, E. Miyazaki, T. Yamamoto, K. Takimiya, *Org. Lett.* 2007, **9**, 4499.
4 P. Gao, D. Beckmann, H. N. Tsao, X. Feng, V. Enkelmann, W. Pisula, K. Müllen, *Chem. Commun.* 2008, 1548.
5 D. Li, Y. Yuan, H. Bi, D. Yao, X. Zhao, W. Tian, Y. Wang, H. Zhang, *Inorg. Chem.* 2011, **50**, 4825.
6 Y.-L. Chen, C.-Y. Chang, Y.-J. Cheng, C.-S. Hsu, *Chem. Mater*. 2012, **24**, 3964.
7 J.-S. Wu, Y.-Y. Lai, Y.-J. Cheng, C.-Y. Chang, C.-L. Wang, C.-S. Hsu, *Adv. Energy Mater.* 2013, **3**, 457.
8 H. Chen, W. Delaunay, J. Li, Z. Wang, P.-A. Bouit, D. Tondelier, B. Geffroy, F. Mathey, Z. Duan, R. Réau, M. Hissler, *Org. Lett*. 2013, **15**, 330.
9 a) M. D. Visco, J. M. Wieting, A. E. Mattson, *Org. Lett.* 2016, **18**, 2883; b) D. Leifert, A. Studer, *Org. Lett.* 2015, **17**, 386; c) E. Pusztai, I. S. Toulokhonova, N. Temple, H.Albright, U. I. Zakai, S. Guo, I. A. Guzei, R. Hu, R. West, *Organometallics* 2013, **32**, 2529.
10 R. Gu, A. Hameurlaine, W. Dehaen, *J. Org. Chem.* 2007, **72**, 7207.
11 K. Kawaguchi, K. Nakano, K. Nozaki, *J. Org. Chem.* 2007, **72**, 5119;
12 D. Hanifi, A. Pun, Y. Liu, *Chem. Asian J*. 2012, **7**, 2615;
13 M. Onoe, K. Baba, Y. Kim, Y. Kita, M. Tobisu, N. Chatani, *J. Am. Chem. Soc.* 2012, **134**, 19477.
14 Y. Liang, W. Geng, J. Wei, Z. Xi, *Angew. Chem. Int. Ed.* 2012, **51**, 1934; *Angew. Chem.* 2012, **124**, 1970.
15 X. Z. Zhu, H. Tsuji, K. Nakabayashi, S.-I. Ohkoshi, E. Nakamura, *J. Am. Chem. Soc.* 2011, **133**, 16342.
16 a) X. Zhu, C. Mitsui, H. Tsuji, E. Nakamura, *J. Am. Chem. Soc.* 2009, **131**, 13596; b) X. Zhu, H. Tsuji, J. T. López Navarrete, J. Casado, E. Nakamura, *J. Am. Chem. Soc.* 2012, **134**, 19254.
17 S. Anderson, P. N. Taylor, G. L. B. Verschoor, *Chem. Eur. J.* 2004, **10,** 518;
18 a) H. Tsuji, C. Mitsui, L. Ilies, Y. Sato, E. Nakamura, J. Am. Chem. Soc. 2007, 129, 11902; b) H. Tsuji, C. Mitsui, Y. Sato, E. Nakamura, Adv. Mater. 2009, 21, 3776;
19 a) O. Gidron, Y. Diskin-Posner, M. Bendikov, *J. Am. Chem. Soc*. 2010, **132**, 2148; b) O. Gidron, A. Dadvand, Y. Sheynin, M. Bendikov, D. F. Perepichka, *Chem. Commun.* 2011, **47**, 1548; c) O. Gidron, A. Dadvand, W.-H. Sun, I. Chung, L. J. W. Shimon, M. Bendikov, D. F. Perepichka, *J. Mater. Chem.* 2013, **1**, 4358.
20 L. C. Li, S. H. Li, C.-H. Zhao, C.-H. Xu, *Eur. J. Inorg. Chem*. 2014, 1880.
21 K. Mitsudo, S. Tanaka, R. Isobuchi, T. Inada, H. Mandai, T. Korenaga, A. Wakamiya, Y. Murata, S. Suga, *Org. Lett*. 2017, **19**, 2564.
22 a) S. Yamaguchi, K. J. Tamao, *Organomet. Chem.* 2002, **653**, 223; b) S. Yamaguchi, K. Tamao, *Chem. Lett.* 2005, **34**, 2.
23 S. H. Lee, B.-B. Jang, Z. H. Kafafi, *J. Am. Chem. Soc.* 2005, **127**, 9071.
24 K. L. Chan, M. J. McKiernan, C. R. Towns, A. B. Holmes, *J. Am. Chem. Soc.* 2005, **127**, 7662.
25 H. Xiao, H. Shen, Y. Lin, J. Su, H. Tian, *Dyes Pigm.* 2007, **73**, 224.
26 a) S. Yamaguchi, K. Tamao, *Bull. Chem. Soc. Jpn.* 1996, **6**9, 2327; b) K. Tamao, M. Uchida, T. Izumizawa, K. Furukawa, S. Yamaguchi, *J. Am. Chem. Soc.* 1996, **118**, 11974; c) S. Yamaguchi, T. Endo, M. Uchida, T. Izumizawa, K. Furukawa, K. Tamao, *Chem.-Eur. J.* 2000, **6**, 1684.
27 a) S. Yamaguchi, C.-H. Xu, K. Tamao, *J. Am. Chem. Soc.* 2003, **125**, 13662; b) C.-H. Xu, A. Wakamiya, S. Yamaguchi. *J. Am. Chem. Soc.* 2005, **127**, 1638.
28 a) C.-H. Xu, A. Wakamiya, S. Yamaguchi, *Org. Lett.* 2004, **6**, 3707; b) L. C. Li, J. F. Xiang, C.-H. Xu, *Org. Lett.* 2007, **9**, 4877.
29 a) T. Agou, J. Kobayashi, T. Kawashima, *Org. Lett.* 2006, **8**, 2241; b) T. Agou, J. Kobayashi, T. Kawashima, *Chem. Eur. J.* 2007, **13**, 8051.
30 T. Matsuda, S. Kadowaki, T. Goya, M. Murakami, *Org. Let*t. 2007, **9**, 133.
31 M. Shimizu, K. Mochida, T. Hiyama, *Angew. Chem. Int. Ed.* 2008, **47**, 9760; *Angew. Chem.* 2008, **120**, 9906.
32 W. Weymiens, M. Zaal, J. C. Slootweg, A. W. Ehlers, K. Lammertsma, *Inorg. Chem.* 2011, **50**, 8516.
33 Y. Liang, S. Zhang, Z. Xi, *J. Am. Chem. Soc.* 2011, **133**, 9204.
34 a) S.-F. Yuan, S. D. Bai, D.-S. Liu, W.-H. Sun, *Organometallics*, 2010, **29**, 2132; b) S.-F. Yuan, T. Duan, L. J. Wang, X. H. Wei, X. X. Wang, W.-H. Sun, *Inorg. Chim. Acta,* 2017, **466**, 497; c) S.-F.Yuan, X. H. Wei, H. B. Tong, L. P. Zhang, D. S. Liu, W.-H. Sun, *Organometallics*, 2010, **29**, 2085; d) S.-F. Yuan, S. D. Bai, H. B. Tong, D.-S. Liu, W.-H. Sun, *Inorg. Chim. Acta*, 2011, **370**, 215; f) S.-F. Yuan, L. J. Wang, Q. Y Zhang, W.-H. Sun, *Prog. Chem.,* 2017, **29**, 1462; g) S.-F. Yuan, L. P. Zhang, D. S. Liu, W.-H. Sun, *Macromol. Res.*, 2010, **18**, 690.
35 Z. Li, W.-H. Sun, X. Jin, C. Shao, *Synlett*, 2001, 1947.
36 B. P. Jacobs, P. T. Wolczanski, E. B. Lobkovsky, *Inorg. Chem*. 2016, **55**, 4223.
37 Z. Xi, R. Fischer, R. Hara, W.-H. Sun, Y. Obora, N. Suzuki, R. Nakajima, T. Takahashi, *J. Am. Chem. Soc.,* 1997, **119**, 12842.
38 (a) G. M. Sheldrick, SADABS Correction Software; University of Göttingen, Göttingen, Germany, 1996; (b) G. M. Sheldrick, SHELX-97, Program for the Solution of Crystal Structures; University of Göttingen, Göttingen, Germany, 1997; (c) O. V. Dolomanov, L. J. Bourhis, R. J. Gildea, J. A. K. Howard, H. Puschmann, *J. Appl. Cryst.*, 2009, **42**, 339.
39 SHELXTL, Program for Crystal Structure Refinement; Bruker Analytical X-ray Instruments Inc., Madison, WI, 1998.